Selective Photoaffinity Labeling of Acetylcholine Receptor Using a Cholinergic Analogue†

V. Witzemann and M. A. Raftery*

ABSTRACT: A bisazido derivative was synthesized from bis(3-aminopyridinium)-1,10-decane diiodide and it was shown that it was bound ($K_D \simeq 2.2$ μM) specifically to purified acetylcholine receptor and fulfilled the requirements for a photoaffinity label. Like the parent compound the derivative could transform membrane-bound receptor from a low ligand affinity conformation(s) to a high ligand affinity form(s), a transition which is thought to resemble desensitization processes observed in vivo. Photolysis of ^{3}H-labeled bisazido reagent was carried out in the presence of the receptor. After dodecyl sulfate–polyacrylamide gel electrophoresis of labeled purified receptor two of the four subunits (mol wt 40 000 and 60 000) contained 90% of the bound radioactivity while for membrane-bound receptor the subunits of mol wt 40 000 and 50 000 were labeled. The results favor the assumption that the specific ligand binding sites are located on mol wt 40 000 subunits and labeling of the other subunits reflects (a) their proximity to the ligand-binding site and (b) alterations in subunit topography between membrane-bound and solubilized states.

The nicotinic acetylcholine receptor (AcChR)[1] protein is located in the postsynaptic membrane of the neuromuscular junction and of some other synapses and its interaction with the neurotransmitter acetylcholine is believed to be the primary event leading to depolarization of the membrane. Reports of receptor purification have appeared, as well as of structural and functional investigations (for reviews see Rang, 1975; Cohen & Changeux, 1975) but despite a large number of studies, our understanding of structural properties of this receptor is still rather limited.

The receptor protein extracted from the electric organ of *Torpedo californica* has been shown to have a molecular weight of about 400 000 (Vandlen & Raftery, 1977) and the number and molecular weights of the receptor subunits could be determined if proteolytic degradation during isolation and workup was excluded. Under these conditions a well-resolved pattern of four polypeptide bands was observed with apparent molecular weights of 40 000, 50 000, 60 000, and 65 000 (Vandlen et al., 1976). The function of the different polypeptides is, however, not yet clear. The 40 000-dalton species has been implicated in α-Bgt binding activity (Hucho et al., 1976; Witzemann and Raftery, 1977). After reduction with dithiothreitol the affinity label MBTA, a cholinergic antagonist, labeled the 40 000-dalton species and in addition partially reduced toxin binding (Weill et al., 1974). More recently it has been shown that the cholinergic agonist, bromoacetylcholine, also reacts specifically with the 40 000-dalton subunit in dithiothreitol-treated AcChR (Hsu and Raftery, unpublished results). These experiments demonstrated that the 40 000-dalton polypeptide that binds α-Bgt has a binding site for small ligands and that for each affinity-label binding site two α-Bgt binding sites exist. In this laboratory it was shown (Raftery et al., 1975) that α-Bgt binds to two populations of receptor sites in purified AcChR, half of which bind ligands such as AcCh, *d*-tubocurarine, and decamethonium with high affinity. This half-site phenomenon was also clearly demonstrated using the fluorescent decamethonium analogue DAP (Martinez-Carrion & Raftery, 1973). More recently we have shown (Sator et al., 1977) that MBTA labeling and DAP binding are not competitive processes. To obtain further information about the DAP binding sites of the AcChR the bisazido derivative of DAP was synthesized for use as a photoaffinity label. (For a review of such photoaffinity reagents see Knowles, 1972.) Since under certain conditions DAP occupies half of the toxin binding sites almost exclusively it was of interest to (1) determine on which of the four types of subunits the binding sites are located and (2) to learn more about functional and topographical aspects of the different AcChR subunits.

Experimental Section

Materials. *Torpedo californica* were obtained locally in Pacific waters. Receptor-enriched membrane fragments were prepared and assayed for α-Bgt binding sites as described previously (Duguid & Raftery, 1973; Reed et al., 1975). AcChR was isolated and purified as described by Vandlen et al. (1976). DAP was synthesized as described by Mooser et al. (1972), using a molar ratio of 3-aminopyridine to 1,10-diiododecane of 5.9:1 instead of 8.5:1 and refluxing in the dark for 70 h with dry distilled acetone. Crystallization was carried out from ethanol. The yield was 77% and the yellowish white needles melted at 180–181 °C. For synthesis of the bisazido derivative 1 g of DAP was dissolved in 20 mL of methanol and 5 mL of concentrated HCl and this solution was kept below 5 °C by cooling with an ice/salt mixture. Under vigorous stirring 4 mL of a 2 M $NaNO_2$ solution was added dropwise over a period of 10 min followed by dropwise addition of 5 mL of a 2 M NaN_3 solution within 3 min, again under vigorous stirring. The reaction mixture was then stirred for about 1 h at 5 °C. Besides the clear yellow solution, some oily compound was formed which was not characterized further because of obvious impurities shown by UV absorption spectroscopy. The reaction product in the methanolic solution was precipitated by addition

† From the Church Laboratory of Chemical Biology, Division of Chemistry and Chemical Engineering, California Institute of Technology, Pasadena, California 91125. *Received July 6, 1977.* Supported by a Fellowship from the Deutsche Forschungsgemeinschaft (to V.W.), by U.S. Public Health Service Grant No. NS-10294, and by a grant from the Sloan Foundation. This paper is Contribution No. 5606 from Church Laboratory of Chemical Biology.

[1] Abbreviations used are: AcChR, acetylcholine receptor; α-Bgt, α-bungarotoxin; MBTA, 4-(*N*-maleimido)benzyltrimethylammonium iodide; DAP, bis(3-aminopyridinium)-1,10-decane diiodide; DAPA, bis(3-azidopyridinium)-1,10-decane perchlorate; UV, ultraviolet; IR, infrared; NMR, nuclear magnetic resonance; TLC, thin-layer chromatography; DEAE, diethylaminoethyl; CARB, carbamoylcholine.

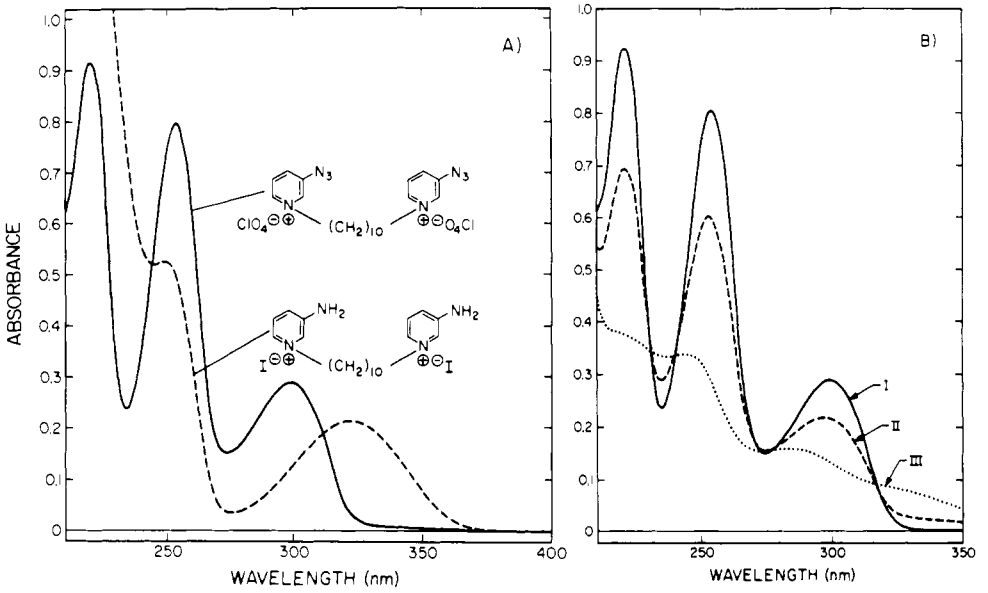

FIGURE 1: (A) Absorption spectra of DAPA and DAP; DAPA (3.2×10^{-5} M) and DAP (3.2×10^{-5} M) in 10^{-3} M sodium phosphate buffer (pH 7.5) at room temperature. (B) Change of absorption spectrum of DAPA after irradiation. DAPA (3.2×10^{-5} M) in 10^{-3} M sodium phosphate buffer (pH 7.5) was irradiated at room temperature with short-wavelength light (see Methods): (I) no irradiation; (II) after 30 s irradiation; (III) after 5 min irradiation.

of $NaClO_4$. The precipitate was dissolved in acetone with gentle heating to remove inorganic salt. After removal of the acetone the residual product was dissolved in hot ethanol and freed from insoluble material. Slow cooling resulted in formation of crystals. Ethanol was used for recrystallization.

Comparison of the UV absorption spectra of DAP and the new product revealed that the absorption maximum at 322 nm due to the NH_2 groups of DAP was completely substituted by a new maximum at 299 nm ($\epsilon = 8.9 \times 10^3$ M^{-1} cm^{-1}) indicative of the existence of azide groups (Knowles, 1972). Other absorption maxima for the new compound occurred at 254 and 220 nm (Figure 1A). Irradiation with UV light caused an immediate decrease of the maxima of the UV absorption (Figure 1B), indicating not only the decomposition of the azide groups but also dramatic changes in the aromatic system. A commercial UV lamp served as a light source (mineral light UVSL-25, Ultra-Violet Products, Inc., San Gabriel, Calif.) with a short-wavelength range (~250-300 nm) and a long-wavelength range (~≥300 nm). No attempts were made to characterize the decomposition product which precipitated in aqueous buffers after prolonged photolysis. The IR spectrum (KBr pellet) showed the characteristic azide absorption at 2130 cm^{-1}, which disappeared completely after irradiation. Elemental analysis supported the evidence from the spectral results that bis(3-azidopyridinium)-1,10-decane perchlorate was obtained. Anal. Calcd for $C_{20}H_{28}N_8Cl_2O_8$: C, 41.46; H, 4.87; N, 19.33. Found: C, 41.63; H, 4.80; N, 18.54.

Further support for bisazido product formation was obtained from NMR spectroscopy; using Me_2SO-d_6 as solvent the sharp signals of the aromatic amino group protons of DAP were completely absent in the azide, whereas all carbon-bonded protons could be assigned. DAPA was tritiated by the Wilzbach method (by ICN Corp.) to yield [^{3}H]DAPA. After several recrystallizations from ethanol the specific activity was 50 Ci/mol and the reagent was radiochemically pure as shown spectroscopically and upon thin-layer chromatography on Eastman Kodak silica gel sheets (using as solvent acetone-ethanol-H_2O-concentrated HCl, 15:5:2:0.5), R_f 0.75. [^{3}H]DAPA migrated with an R_f equal to unlabeled DAPA and contained the total radioactivity applied to the TLC plate.

Methods. [^{125}I]-α-Bgt-AcChR complex formation was determined using a DEAE filter disc assay procedure (Schmidt and Raftery, 1973). The precise conditions for each experiment are given in the figure legends.

Dodecyl sulfate-polyacrylamide gel electrophoresis was performed as described by Vandlen et al. (1976). Photolabeling was carried out at room temperature, since no significant difference was found when photolysis was conducted at 4 °C. Irradiation with the short-wavelength range of the UV lamp used and irradiation times of 1-2 min were more efficient than irradiation with the long-wavelength range and irradiation times up to 10 min (Figure 6). For photolysis conditions applied see the figure legends. Samples were in all quartz cells with a pathlength of 1 cm and were placed 0.5 cm from the light source. Photolabeling of membrane fragment solutions was carried out under gentle stirring.

Results

DAPA Interactions with Membrane-Bound AcChR. (a) Reversible Interaction. Binding of DAPA to AcChR-enriched membranes was studied indirectly by virtue of its ability to affect the time course of [^{125}I]-α-Bgt-receptor complex formation in a manner similar to DAP and other cholinergic ligands (Raftery et al., 1975). In addition, the extent of DAPA-induced inhibition increased with time of exposure of the membrane preparation to the ligand prior to addition of the toxin (Figure 2A). This is analogous to previously reported in vitro studies on a ligand-induced high-affinity form(s) of *Torpedo* AcChR using agonists (Weber et al., 1975; Weiland et al., 1976; Lee et al., 1977) or antagonists (Lee et al., 1977; Quast et al., 1977). Following preincubation, removal of DAPA by dilution resulted in a preparation with a time course for [^{125}I]-α-Bgt-AcChR complex formation identical with that obtained for AcChR membranes never exposed to the ligand, thus demonstrating that the AcChR in either the low ligand affinity form (untreated with DAPA) or the high ligand affinity form (immediately after dilution of the DAPA prein-

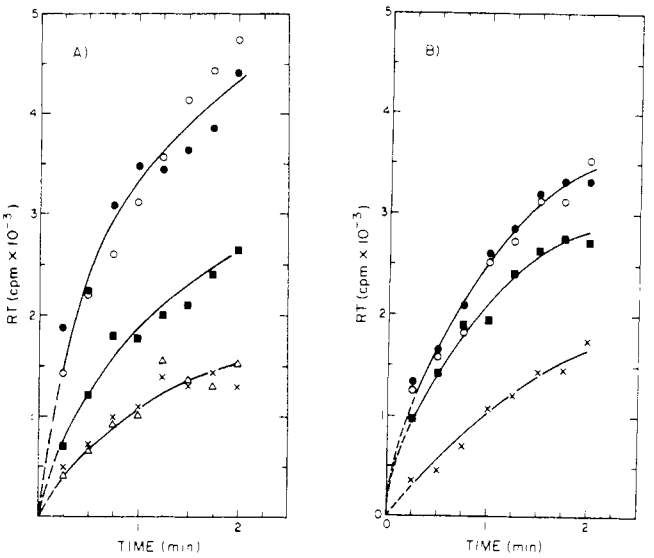

FIGURE 2: (A) Interaction of DAPA with AcChR-rich membrane fragments. Membrane fragments were incubated in Ringer's buffer in the presence and absence of DAPA (10^{-5} M) for 15 min at room temperature. After irradiation with the long-wavelength range of the lamp used (see Methods) for 10 min the membrane fragments were diluted (40×) and the time course of [^{125}I]-α-Bgt binding was measured. The initial toxin concentration was 2.6×10^{-7} M. The final AcChR concentration (in toxin binding sites) was 0.6×10^{-7} M: toxin binding to membrane fragments after irradiation in the absence of DAPA (●); membrane fragments were incubated with DAPA, but not irradiated and toxin binding was measured immediately after dilution (○); membrane fragments were treated as in (○), but toxin binding was determined after dilution into 2×10^{-5} M DAPA (×); membrane fragments were irradiated in the presence of DAPA and toxin binding was determined after dilution (△); toxin binding to membrane fragments after dilution in the presence of DAPA (■). (B) Photoaffinity labeling of AcChR-rich membrane fragments in the absence and presence of DAP. AcChR-rich membrane fragments in Ringer's buffer were incubated with 5×10^{-6} M DAPA for 10 min at room temperature followed by irradiation for 2 min with the short-wavelength range of lamp used; see Methods (×); membrane fragments were treated as above but in the presence of 10^{-5} M DAP (■). Controls: membrane fragments incubated in the absence (○) or presence (●) of DAPA (5×10^{-6} M) without irradiation. [^{125}I]-α-Bgt binding was determined after extensive dialysis (Ringer's buffer), where the initial toxin concentration was 2.6×10^{-7} M. The AcChR concentration in toxin binding sites was 0.5×10^{-7} M.

cubated preparation) appeared to have closely similar if not identical kinetics of reaction with α-Bgt.

(b) Covalently Bound DAPA. Following irradiation of DAPA in the presence of AcChR-enriched membranes the preparation appeared to be in the high-affinity form for ligand (Figure 2A), as judged by the time course of [^{125}I]-α-Bgt-AcChR complex formation. Upon dilution of the sample this time course did not change as it had in the case of the nonirradiated parallel experiment discussed before. Control experiments, using AcChR membranes irradiated under identical conditions but in the absence of DAPA, demonstrated that irradiation alone had no effect on [^{125}I]-α-Bgt-AcChR complex formation. The specific incorporation of DAPA at the DAP binding region is demonstrated in Figure 2B. Irradiation of membrane fragments with azide was carried out in the presence of DAP and after extensive dialysis to remove DAP and unbound azide decomposition products the toxin binding time course of these treated membrane fragments was essentially the same as the time course of untreated fragments. In the control experiment for this effect, i.e., no DAP included, the incorporation of azide was clearly shown by the reduction of the time course of receptor–toxin complex formation (Figure 2B). (The degree of modification in this case was apparently not as high as in the former experiment (Figure 2A), due to different initial azide concentrations.) However, contrary to the observed inhibition of the toxin binding rate after covalent binding of DAPA, no significant difference was found between azide-containing and native receptor enriched membranes in terms of the amount of total toxin bound at equilibrium ($t = \infty$), indicating that ternary complexes of AcChR, [^{125}I]-α-Bgt, and photolyzed DAPA were formed.

DAPA Binding to Purified AcChR. (a) DAPA as Reversible Ligand. From inhibition of the toxin binding time course with DAPA present a $K_d = 2.5$ μM was determined for this ligand binding to purified AcChR (Figure 3B). Compared to the K_d of DAP (0.4 μM) measured under the same conditions the binding was about sixfold weaker. Previously it was shown that DAP binds to only half the toxin binding sites of purified AcChR (Martinez-Carrion and Raftery, 1973; Raftery et al., 1975). As shown in Figure 3A for inhibition of [^{125}I]-α-Bgt binding by DAPA, the slopes for the first half of the toxin-binding reaction remained (in the concentration range used) nearly constant, whereas the slopes for the second half were greatly decreased. This corresponds well with data for the parent ligand DAP (Raftery et al., 1975) and demonstrates the preferential strong binding of DAPA to half of the toxin binding sites.

(b) Covalent Binding of DAPA. Purified receptor was labeled with DAPA by irradiation and excess reagent and decomposition products were removed by dialysis. In studies of [^{125}I]-α-Bgt binding to this preparation, half of the toxin binding reaction was inhibited (Figure 4), i.e., the toxin kinetics showed two components of equal magnitude, with the slower component being inhibited. When photolysis of the DAPA-AcChR complex was carried out in the presence of 10^{-4} or 5×10^{-5} M DAP (Figure 4) and ligands were removed by dialysis the toxin binding kinetics indicated that DAP protected efficiently against incorporation of DAPA into the purified AcChR. Other ligands such as decamethonium or hexamethonium also afforded protection but were less effective than DAP, whereas CARB had very little influence on the degree of incorporation and only at concentrations above 1 mM was significant inhibition of labeling obtained (not shown). As already found with membrane fragments the amount of toxin bound at equilibrium was identical for photolabeled or native receptor, indicating that the covalent incorporation of the ligand could slow the kinetics of toxin–receptor complex formation but could not prevent it.

Radiolabeled DAPA. Purified AcChR was irradiated in the presence of [^{3}H]DAPA and these photolyzed samples were analyzed by polyacrylamide gel electrophoresis in sodium dodecyl sulfate. A polypeptide composition of four major species was observed as previously found for unmodified receptor, with molecular weights of 40 000, 50 000, 60 000, and 65 000 (Figure 5A). Two of these polypeptides, the 40 000- and 60 000-dalton species, were mainly labeled (Figure 5B). The specificity of this labeling was determined by irradiation of receptor and [^{3}H]DAPA in the presence of α-Bgt or DAP. In both cases incorporation of radioactivity was dramatically decreased in the 40 000- and 60 000-dalton bands while the minor labeling of the 50 000- and 65 000-dalton bands was decreased by a much lesser extent (Figure 5B). CARB also afforded some protection at high concentration (10^{-3} M, ~20-fold in excess of its K_d) but was not as effective as other ligands. The dependence of incorporation of radiolabel on the azide concentration and on irradiation time (Figure 6A,B) was investigated to show whether the DAPA site was saturable and whether the kinetics of photolabeling showed saturation. As a function of azide concentration (Figure 6A) preferential

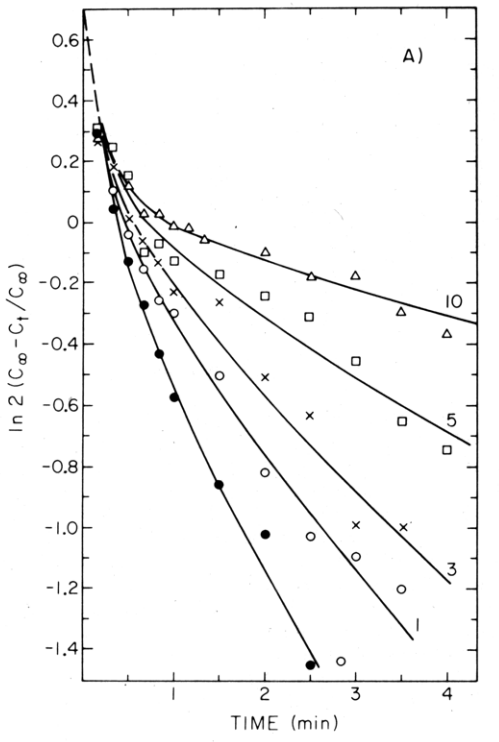

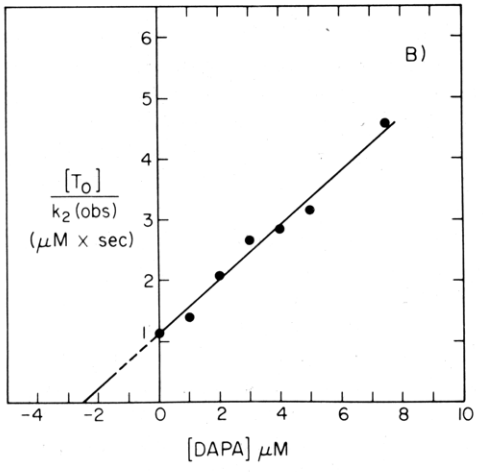

FIGURE 3: (A) Kinetics of [^{125}I]-α-Bgt binding to AcChR in the presence of DAPA. The initial toxin concentration was 1.3×10^{-7} M and the concentration of toxin binding sites was 0×10^{-7} M. Only the slow toxin binding component (see Raftery et al., 1975) was affected by the presence of the ligand. Reactions were carried out in buffers containing 10 mM sodium phosphate and 100 mM NaCl at pH 7.4 at room temperature. Solid lines are obtained from a nonlinear least-squares fit of the data to $C_t = C_0 (2 - e^{-k_1 t} - e^{-k_2 t})$ (Raftery et al., 1975) assuming two types of noninteracting toxin binding sites. Numbers next to the curves indicate DAPA concentrations used (0, 1, 3, 5, and 10×10^{-6} M): C_t = concentration of bound [^{125}I]-α-Bgt measured at time t; C_0 = half-maximum concentration of toxin bound, when reaction reached completion; k_1 = rate constant for [^{125}I]-α-Bgt binding to the half of the toxin sites not occupied by the ligand; k_2 = rate constant for binding of [^{125}I]-α-Bgt to the site occupied by the ligand (DAPA); C_∞ = the amount of [^{125}I]-α-Bgt bound at equilibrium. (B) Dissociation constant for DAPA binding to AcChR. k_2 was obtained from the equation shown in the legend to A: T_0 = initial [^{125}I]-α-Bgt concentration (= 1.3×10^{-7} M). A K_d of 2.5×10^{-6} M was determined.

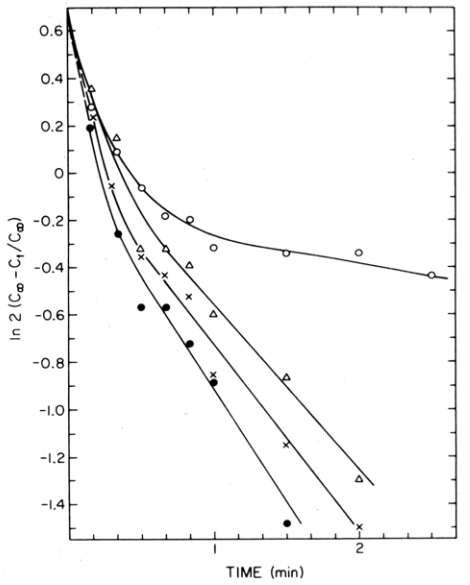

FIGURE 4: [^{125}I]-α-Bgt binding to covalently labeled AcChR. AcChR (2×10^{-6} M) was irradiated with the short-wavelength lamp (Methods) for 2 min at room temperature in the presence of DAPA (2×10^{-5} M) (○); the same experiment was done in the presence of 5×10^{-5} M DAP (△) or 10^{-4} M DAP (×); control, unlabeled AcChR in the absence of ligands (●). Toxin time courses were measured after extensive dialysis.

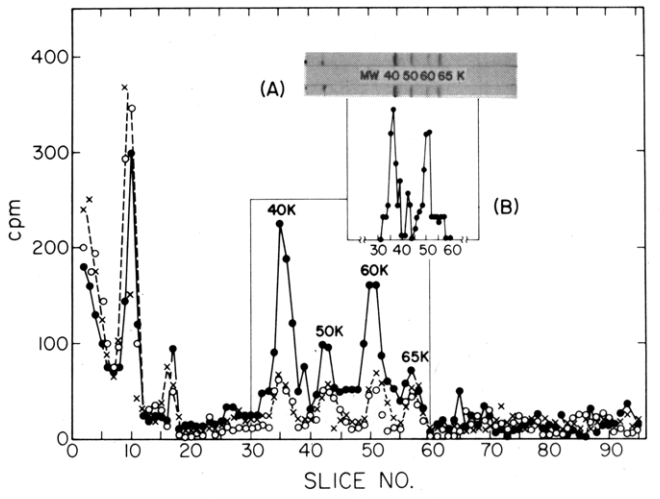

FIGURE 5: Distribution of radioactivity after separation of purified AcChR subunits covalently labeled with [^{3}H]DAPA. Gels were cut into 1-mm slices beginning at the dye front and radioactivity was measured. The radioactivity next to the dye front (fractions 9–11) was probably due to labeled phospholipids (Bayley and Knowles, 1977) and free azide decomposition products. AcChR (1.2 μM) was photolabeled in the presence of 11 μM DAPA in the absence of other ligands or in the presence of 60 μM DAP (×) or 7.5 μM α-Bgt (○). (Insert A) (Top) Purified AcChR. (Bottom) Purified AcChR reacted with DAPA. Insert B shows radioactivity incorporated into AcChR subunits after subtraction of nonspecific labeling which was determined from experiments where specific labeling was eliminated due to the presence of DAP or toxin. The protein bands shown (using Coomassie blue staining) correspond well with the distribution of radioactivity. Comparing the areas of the radioactivity profile for each subunit and normalizing for the molecular weights showed that the mol wt 40 000 subunit contained 48% of total AcChR-bound radioactivity, the mol wt 50 000 subunit 5%, the mol wt 60 000 subunit 43%, and the mol wt 65 000 subunit 4%.

labeling of the 40 000- and 60 000-dalton subunits was obtained, reflecting specific photolabeling as compared with nonspecific incorporation of azide into the 50 000- and 65 000-dalton polypeptides. Saturation of the specific ligand sites is shown in Figure 7. The photochemical reaction also followed saturation kinetics (Figure 6B), for which short-wavelength irradiation was more efficient than long-wavelength irradiation. By comparing the half-times for receptor labeling and decomposition of azide alone it was demonstrated that the sensitivity of DAPA to irradiation was significantly increased when bound to the receptor. Half-times for decomposition of azide alone with short-wavelength irradiation were

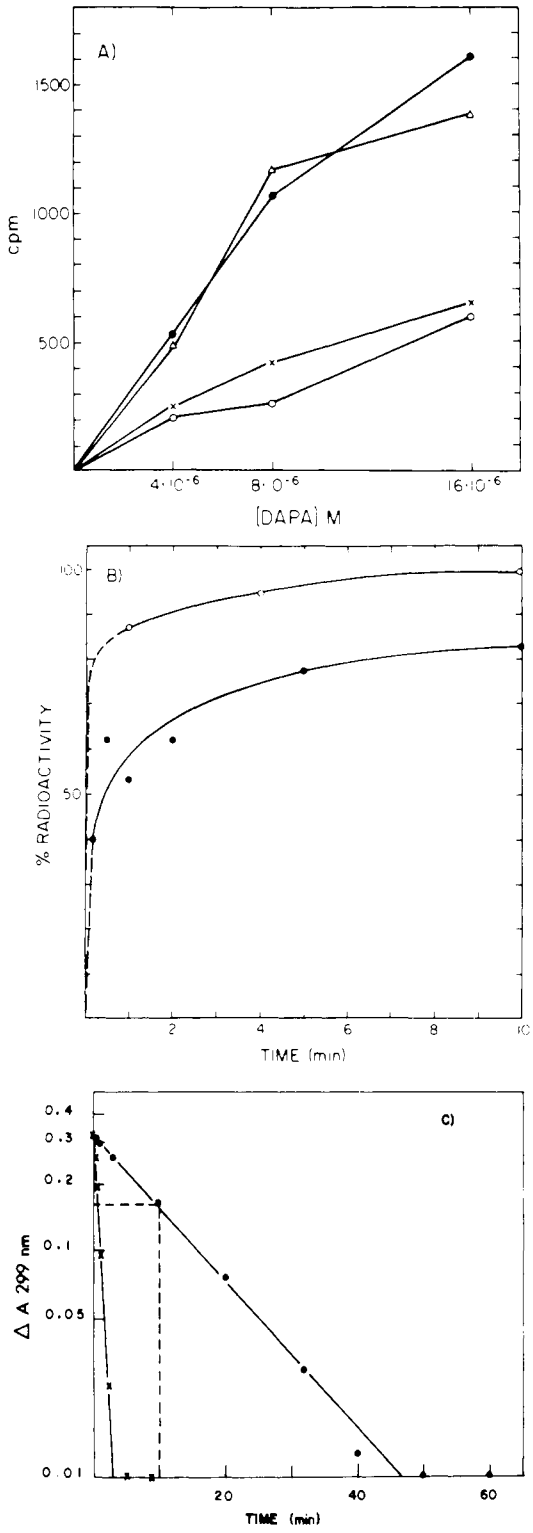

FIGURE 6: (A) Degree of [^{3}H]DAPA labeling as a function of [^{3}H]-DAPA concentration. AcChR (1.2 μM) was irradiated (2 min, with the short-wavelength lamp (see Methods) at room temperature) in the presence of 4, 8, and 16 μM DAPA. After sodium dodecyl sulfate-gel electrophoresis of 0.1-mL aliquots the gels were sliced and radioactivity bound per subunit plotted vs. [^{3}H]DAPA concentrations (curves are not corrected for nonspecific labeling): mol wt 40 000 (●); mol wt 50 000 (×); mol wt 60 000 (△); mol wt 65 000 subunits (○). (B) Dependence of labeling on irradiation time and wavelength. Irradiation with long-wavelength range (●) and short-wavelength range of lamp used (○) (see Methods). Short-wavelength irradiation was more efficient, so that shorter irradiation times could be used. (C) Photolysis of DAPA. The decrease in the absorbance at 299 nm characteristic of azide groups was measured at the times indicated until there was no further change. Half-times of decomposition were 40 s with the short-wavelength lamp (×) and 10 min with the long-wavelength lamp (●).

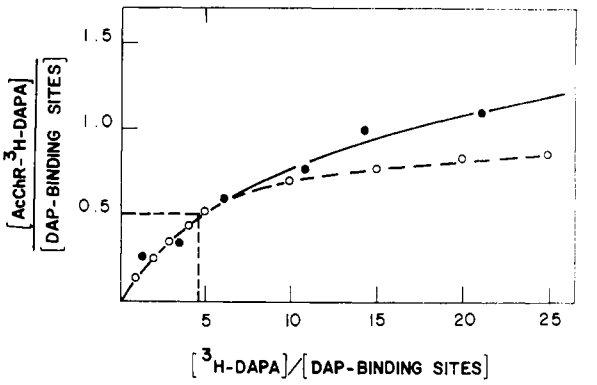

FIGURE 7: Dependence of photolabeling on [^{3}H]DAPA concentration determined by a DEAE filter disc method. AcChR was irradiated (1 min, with the short-wavelength lamp at room temperature) in the presence of [^{3}H]DAPA concentrations ranging from 0.8 to 16.5 μM: (●) experimental points; (○) calculated for K_d = 1.9 μM. The ordinate represents the concentration of AcChR sites modified by [^{3}H]DAPA divided by the number of DAP binding sites present [AcChR-[^{3}H]DAPA]/[DAP-binding sites]. The abscissa represents the concentrations of [^{3}H]DAPA used relative to the number of DAP binding sites present, i.e., the excess of [^{3}H]DAPA used over binding sites present and is shown as [[^{3}H]-DAPA]/[DAP sites]. DAP-binding sites correspond to half of the toxin sites, [DAP-binding sites] = 0.47 μM. The concentration of the AcChR-[^{3}H]DAPA complex formed was estimated from the radioactivity bound.

40 s, or 10 min using the long-wavelength range. (Decomposition was followed by measuring the decrease of the 299-nm band as an indicator of azide groups (Figure 6C).) Especially in the case of long-wavelength irradiation the different rates of receptor labeling and decomposition became obvious where the labeling occurred at least 5 to 10 times faster in the presence of AcChR.

Since DAPA has two reactive azide groups it was conceivable that reaction with different subunits would result in cross-linking. It was not possible to detect even small amounts of such cross-linking under the conditions used, since the yield of radioactivity after slicing and solubilizing the gels was low. Using five- to tenfold higher receptor concentrations and tenfold higher azide concentrations some radioactivity was associated with higher molecular weight species (not shown). However, it was difficult to decide whether this was due to random labeling of some minor higher molecular weight components still present in the purified AcChR preparation or resulted from AcChR subunits cross-linked by azide.

Using a DEAE disc assay to bind AcChR as described for [^{125}I]-α-Bgt-AcChR binding assays (Schmidt and Raftery, 1973), the amount of covalently bound DAPA was measured as a function of initial DAPA concentration (Figure 7). With increasing [^{3}H]DAPA concentrations the amount of nonspecific labeling increased and the estimation of the concentration of the AcChR-[^{3}H]DAPA complex became rather imprecise. This is shown by the fact that the binding curve exceeded the value of 1.0 on the ordinate in Figure 7. Assuming two independent DAPA binding sites one can calculate a theoretical saturation curve, which was fitted to the experimental data by varying the K_d values. The best fit was achieved assuming a K_d of 1.9 μM and for the initial phase the correspondence of the experimental and theoretical curves was very good, with an experimentally determined K_d of 2.2 μM. Under the conditions normally used for photolabeling (5–10 μM DAPA) about 70% of the DAPA-binding sites were modified as determined from the plot shown in Figure 7. DAP (in fivefold molar excess over DAPA) protected against photoinduced incorporation of [^{3}H]DAPA to the extent of 60–80%, while

decamethonium and hexamethonium (fivefold molar excess over DAPA) protected to the extent of 40–60 and 20–30%, respectively. Assuming that the theoretical curve in Figure 7 (dashed line) represents specific binding of DAPA and that the higher incorporation of radioactivity found experimentally above 5 μM [^{3}H]DAPA was due to nonspecific incorporation of nitrene residues one can estimate the amount of bound azide per α-Bgt binding site: using modification conditions of [AcChR] = 0.92 μM in toxin binding sites and an azide concentration of 6.6 μM it was found that 0.4 mol of photolabel was incorporated per 1.0 mol of toxin binding sites.

AcChR-enriched membrane fragments were irradiated in the presence of [^{3}H]DAPA and polyacrylamide gel electrophoresis of these samples was performed in sodium dodecyl sulfate (Figure 8) with the AcChR subunits being identified using the polypeptide pattern of an identically treated sample of solubilized purified AcChR as marker. In analyzing the distribution of the bound radioactivity it was found that the 40 000-dalton subunit was labeled and in addition about the same amount of radioactivity was associated with the 50 000-dalton subunit, whereas the 60 000- and 65 000-dalton polypeptides showed only minor labeling, barely significant above the background (Figure 8). This result is in contrast to the findings with purified solubilized AcChR, where the 60 000-dalton polypeptide was labeled to an extent comparable to that of the 40 000-dalton species. To test the specificity of this photolabeling process, membrane fragments were incubated with α-Bgt to block access to all DAP (or DAPA) binding sites. By irradiation of [^{3}H]DAPA in the presence of such protected membrane fragments labeling was prevented almost completely (Figure 8). This was true for the 40 000- as well as the 50 000-dalton subunit. Apparently no cross-linking had occurred in either experiment since no radioactivity was bound to higher molecular weight components.

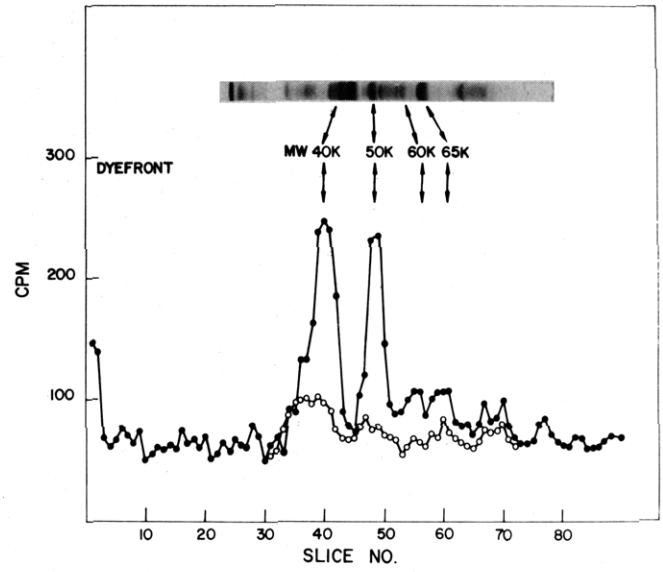

FIGURE 8: Sodium dodecyl sulfate–gel electrophoresis of photolabeled AcChR-rich membrane fragments. Membrane fragments (5×10^{-6} M in α-Bgt binding sites) in Ringer's (pH 7.5) were irradiated in the presence of DAPA (3×10^{-5} M) (●) or they were incubated with α-Bgt (3.2×10^{-5} M) for 20 min at room temperature prior to irradiation in the presence of DAPA (○). Photolysis was carried out at room temperature for 2 min using the short-wavelength lamp (see Methods). The polypeptide pattern of AcChR-rich membrane fragments after sodium dodecyl sulfate–gel electrophoresis is shown, where the arrows indicate the corresponding molecular weights and incorporated radioactivity.

Discussion

The data presented here indicate that the bisazido analogue of DAP satisfied the basic requirements for a photoaffinity label for the AcChR. In terms of its biochemical properties DAPA was very similar to DAP in that it bound to half of the α-Bgt binding sites of the AcChR with much higher affinity than to the other half and the K_d for this strong binding to soluble purified receptor was about 2.5 μM, which presented a six- to eightfold weaker binding than that of the parent compound DAP to the same preparation.

That DAPA binding was competitive with DAP was indicated by its ability to transform membrane fragments in their low ligand affinity form to a form of higher affinity in a manner similar to the DAP (Lee et al., 1977; Quast et al., 1977), and this was further substantiated by the observation that DAP could protect toward incorporation of photolabel in a highly efficient manner.

No covalent labeling of receptor occurred without irradiation and the irradiation procedures in and of themselves did not change the toxin or ligand binding characteristics of the AcChR in membrane-bound or solubilized, purified form if light exposure was carried out in the absence of the azide. No detectable change in subunit composition, e.g. degradation or cross-linking, as a result of irradiation could be observed on sodium dodecyl sulfate–polyacrylamide gel electrophoresis. Furthermore, the kinetics of photolabeling showed saturation and the binding site for the azide was saturable. These observations all suggest that the photoinduced labeling was a specific process.

The result which showed that toxin protected against photolabeling but that on the other hand DAPA once incorporated in the absence of toxin could not prevent ultimate binding of toxin can be explained by assuming that bound DAPA blocks only two anionic sites which are not essential for toxin binding; this means that other additional anionic sites for binding of toxin very likely exist. Therefore, the covalent introduction of the photolabel (nonradiolabeled) could be indirectly observed only by observing the toxin binding time courses, which were significantly decreased, rather than by determination of the [^{125}I]-α-Bgt bound at equilibrium.

Other ligands besides DAP were tested for their protective ability which was found to increase in the order CARB < hexamethonium < decamethonium < DAP. This is consistent with the binding properties of these ligands (Raftery et al., 1974). The smallest effect found with CARB indicated that different anionic sites may exist for the two ligands DAPA and CARB and this result is consistent with other observations made in this laboratory (Raftery et al., 1974; Bode et al., 1977) which led to the suggestion that at least three different types of anionic sites are present, one for binding of AcCh or CARB, while the others complex inorganic cations, or other mono- or divalent ligands.

The purified AcChR was labeled with [^{3}H]DAPA to determine which of the subunits contained the high affinity binding sites and it was shown that the polypeptides of apparent mol wt 40 000 and 60 000 were specifically labeled. The question arising from this is whether both subunits carry specific sites? If such were the case the 60 000 mol wt subunit would have approximately four times as many binding sites as the 40 000-dalton subunit, since the radioactivity associated with both subunits was about the same while the ratio of 40 000 polypeptide chains to 60 000-dalton polypeptide chains, based on Coomassie blue staining after sodium dodecyl sulfate–gel electrophoresis (Raftery et al., 1975), is of the order of 4:1. This seems to be unlikely for several reasons. (a) Four moles of [^{125}I]-α-Bgt binds to *Torpedo californica* AcChR (Raftery et al., 1975), while half this number of sites are occupied by

DAP (see Results). This would imply that the 40 000- and 60 000- dalton species each have one binding site for DAP (or DAPA) and that the dissociation constants were identical, as observed experimentally (Martinez-Carrion and Raftery, 1973; Raftery et al., 1975). (b) There is evidence that α-Bgt binds to the 40 000-dalton polypeptide (Hucho et al., 1976; Witzemann and Raftery, 1977), presumably one toxin molecule to each subunit of mol wt 40 000. If there were specific ligand binding sites on the 60 000-dalton subunit one would not expect that the toxin could protect toward photolabeling, as observed in our experiments. Therefore, the assumption that the azide binding sites and hence the high-affinity ligand binding sites are located on the 40 000-dalton subunits seems more reasonable. Reaction with the 60 000-dalton subunit is then possible because this subunit is close to the DAPA binding area. Nitrene molecules, sufficiently long-lived, could diffuse from the specific DAP or DAPA binding sites and be incorporated into an adjacent 60 000-dalton subunit, reacting with particularly suitable nucleophiles and blocking further access of azide to the DAP binding site. Since there was no significant cross-linking under the experimental conditions used, the binding of ligand to two different anionic sites on different subunits at the same time appears to be unlikely.

The results obtained with [^{3}H]DAPA labeled membrane fragments strongly support the assumption that the 40 000-dalton subunit actually carries the specific binding region for DAPA and therefore for DAP and they also reflect structural features of membrane-bound AcChR. Again, in addition to the 40 000-dalton subunit a second polypeptide, this time of mol wt 50 000, was labeled to about the same extent as the former. Incorporation of radioactivity into both polypeptides could be prevented almost completely if access to the DAPA-binding site was blocked by α-Bgt. Since α-Bgt binds, as noted above, to the 40 000-dalton subunit the specific binding site of DAPA should be located on the same subunit and reaction with the 50 000-dalton subunit could reflect structural proximity of this polypeptide to the specific DAPA-binding area in the membrane-bound AcChR for the same reasons as discussed in the case of solubilized receptor, where the 60 000-dalton subunit seemed to be closely associated with the 40 000-dalton subunit. The fact that labeling occurred on two different polypeptides in addition to common incorporation of [^{3}H]DAPA into the 40 000-dalton subunit, dependent on the conformational state of the AcChR, suggests that the specific binding site of this ligand is actually only on the 40 000-dalton subunit. This interpretation suggests that labeling of the 50 000 or 60 000-dalton polypeptides occurred for structural reasons and not because of specific binding sites on both polypeptides. These results imply that the structural arrangement of the AcChR subunits of membrane-bound receptor differs from the purified, solubilized form.

In conclusion it seems reasonable to suggest that in addition to α-Bgt interacting with the 40 000 mol wt subunits of the AcChR a variety of cholinergic ligands interact with these subunits as well. MBTA can covalently label half of these subunits (Weill et al., 1974) and DAP interacts also with these same polypeptide types (Sator et al., 1977). Labeling by [^{3}H]DAPA of a second polypeptide (60 000 mol wt) of the purified AcChR in solution in addition to the 40 000-dalton subunit indicates that interactions between these two subunits exist within a quarternary ensemble while in the membrane-bound state alterations in such interactions occur. The functional aspects of quaternary structure have yet to be ascertained not only for the 50 000- and 60 000-dalton subunits, but also for the 65 000-dalton polypeptide(s).

References

Bayley, H., & Knowles, J. R. (1977) (in press).

Bode, F., Moody, T., Schimerlik, M., & Raftery, M. A. (1977) manuscript in preparation.

Cohen, F. B., & Changeux, J.-P. (1975) *Ann. Rev. Pharmacol. 15,* 83-103.

Duguid, J. R., & Raftery, M. A. (1973) *Biochemistry 12,* 3693.

Hucho, F., Layer, P., Kiefer, H. R., & Bandini, G. (1976) *Proc. Natl. Acad. Sci. U.S.A.* 73, 2624-2628.

Knowles, J. R. (1972) *Acc. Chem. Res. 5,* 155-160.

Lee, T., Witzemann, V., Schimerlik, M., & Raftery, M. A. (1977) *Arch. Biochem. Biophys. 183,* 57-63.

Martinez-Carrion, M., & Raftery, M. A. (1973) *Biochem. Biophys. Res. Commun. 55,* 1156-1164.

Mooser, G., Schulman, H., & Sigman, D. S. (1972) *Biochemistry 11,* 1595-1602.

Quast, U., Schimerlik, M., Lee, T. Witzemann, V., Blanchard, S., & Raftery, M. A. (1977) *Biochemistry* (in press).

Raftery, M. A., Bode, F., Vandlen, R. L., Chao, Y., Deutsch, J., Duguid, J. R., Reed, K., & Moody, T. (1974) *Biochemistry of Sensory Functions* (Jaenicke, Ed.) p 541, Springer Verlag, New York, N.Y.

Raftery, M. A., Vandlen, R. L., Reed, K. L., & Lee, T. (1975) *Cold Spring Harbor Symp. Quant. Biol. 40,* 193-202.

Rang, H. P. (1975) *Q. Rev. Biophys. 7,* 283-399.

Reed, K., Vandlen, R. L., Bode, J., Duguid, J. R., & Raftery, M. A. (1975) *Arch. Biochem. Biophys. 167,* 138.

Sator, V., Martinez-Carrion, M., & Raftery, M. A. (1977) *Arch. Biochem. Biophys.* (in press).

Schmidt, J., & Raftery, M. A. (1973) *Anal. Biochem. 52,* 349-354.

Vandlen, R. L., & Raftery, M. A. (1977) manuscript in preparation.

Vandlen, R. L., Schmidt, J., & Raftery, M. A. (1976) *J. Macromol. Sci. Chem. A10,* 73-109.

Weber, M., David-Pfeuty, T., & Changeux, J. P. (1975) *Proc. Natl. Acad. Sci. U.S.A. 72,* 3443.

Weiland, G. Gregoria, B., Wee, V. T., Chignell, C. F., & Taylor, P. (1976) *Mol. Pharmacol. 12,* 1091.

Weill, C. H. L., McNamee, M. G., & Karlin, A. (1974) *Biochem. Biophys. Res. Commun. 61,* 997-1003.

Witzemann, V., & Raftery, M. A. (1977) submitted for publication.